International Journal of Bioelectromagnetism *www.ijbem.org*
Vol. 23, No. 1, pp. 5/1 - 4 , July 2021.

A 50 channel optically pumped magnetometer MEG in an externally actively shielded two-layer room

T.H. Sander[a], U. Marhl[b,c], R. Brühl[a], T. Middelmann[a], V. Jazbinšek[c]
[a]Physikalisch-Technische Bundesanstalt, Berlin, Germany
[b]University of Maribor, Maribor, Slovenia
[c]Institute of Mathematics, Physics and Mechanics, Ljubljana, Slovenia

Correspondence: T.H. Sander, Physikalisch-Technische Bundesanstalt, 10587 Berlin
Email: tilmann.sander-thoemmes@ptb.de Website: *www.ptb.de* Phone: +49 30 3481 7436

Abstract. Dynamic variations and slow field drifts exceeding 1 nT can be a challenge for optically pumped magnetometers (OPM) used for magnetoencephalography in existing three layer magnetically shielded rooms. These drifts can drive the sensors into non-linearity or worse, saturate the sensors.

Here we describe that a triple axis active shielding coil system enclosing the outside surfaces of the room is sufficient to allow OPM operation in the linear regime. Auditory evoked fields for two types of sensor placement show the typical bi-hemispheric activation and the dipolar field map on a single hemisphere. Since the OPMs measure two orthogonal components of the field the sensors can be oriented to measure the quasi-radial and a tangential component of the brain activation at the same time. Results show qualitatively the theoretically expected field patterns.

Keywords: Optically pumped magnetometer, magnetoencephalography, shielded room, active shielding, linear operation

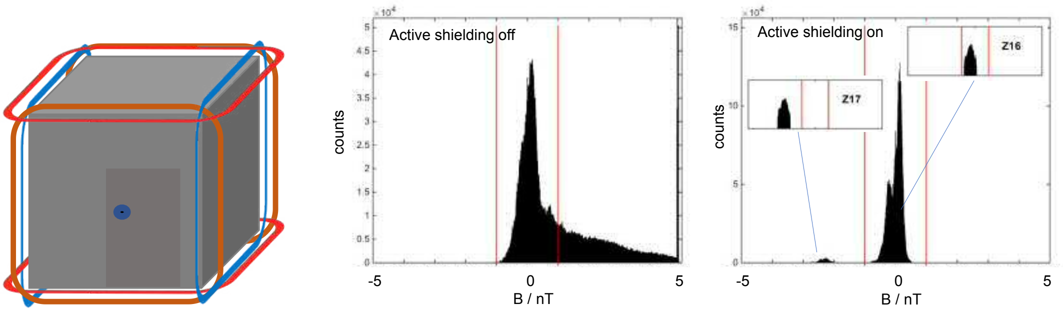

a) b) c)

Figure 1. *a) Sketch of the coils around the edges of the MSR. Coils enclosing opposite sides are connected in series and an active PID three channel electronics drives the coils. Fluxgates (not shown) on three of the surfaces measure the control signal. b) Distribution of OPM signal values for a 30 minute measurement in all 25 z-channels with active shielding not running. Signal values above 1 nT occur frequently and sensors are non-linear in this regime. c) Distribution of OPM signal values for a 30 minute measurement in all 25 z-channels with active shielding running. The insets show a single channel (Z17) not being locked around zero field and a representative channel (Z16) locked to zero and in normal operating mode.*

1. Introduction

Magnetically shielded rooms (MSR) have been complemented successfully by active shielding with coils for a long time (Malmivuo et al., 1987). With the introduction of zero-field optically pumped magnetometers (OPM) the focus shifted to frequencies below 0.1 Hz as the shielding factor of μ-metal drops for low frequencies and the ambient time dependent fields in MSRs can lead to saturation of OPMs (Osborne et al., 2018). In this work a simple triple-axis coil system at the outside edges of a magnetically shielded room is characterized, which allows MEG recordings with zero-field OPMs. This coil system was installed during the installation of the MSR by the supplier. A commercial active add-on shielding system of similar design would probably yield comparable results as only the placing of fluxgates is different between the two designs (ecatalog.elekta.com/neuroscience/

content/pdf/NM23040B External active shielding.pdf). The aim here is not to extend MEG into novel paradigms involving movements (Boto et al., 2018), but to demonstrate standard cognitive neuroscience motivated MEG recordings (Gross 2019) with a seated subject (Sander et al., 2020; Marhl et al., 2021). Additionally, the dual-axis operation mode of commercial OPMs is employed here and tangential brain fields are recorded together with the customary quasi-radial brain fields, where quasi-radial denotes the fields normal to the skull surface.

2. OPM-MEG in a two-layer magnetically shielded room

There exist roughly 100 shielded rooms around the world like the three-layer Ak3b (two-layer μ-metal, one layer with high electrical conductivity; Vacuumschmelze GmbH, Germany). They are optimized for SQUID-MEG and usually do not shield sufficiently below 0.1 Hz to operate the commercial zero-field OPMs employed here (of type QZFM Gen2.0, QuSpin Inc., USA) in their linear regime below 1 nT (Osborne et al., 2018).

While DC-offsets can be compensated by an internal three-axis coil system, a sensor internal compensation of slow variations or drifts is not possible. Thus, if the background field diverges to much from the initial value (>1 nT) the non-linear regime is entered. The non-linear regime can be seen in the signal distribution of the z-axis of 25 OPMs in Fig. 1 b). Field fluctuations of up to 5 nT exist for a considerable part of the distribution which contains the data from a 30-minute empty room recording. The OPM signal distribution shown in Fig. 1 c) was recorded with the triple-axis coils sketched in Fig. 1 a) driven by a PID circuit (stefan-mayer.com) with fluxgate sensors on the cuboid surfaces as control signal. The distribution is in the linear regime except for channel Z17 (enlarged in the inset) not having locked properly for unknown reasons. Improper locking could be detected automatically as an offset, but the functionality to detect it is not yet part of the commercial sensor control software. An example for a sensor operating in the linear regime (Z16) is shown in the second inset in Fig. 1 c).

The 25 OPM sensors were inserted into a helmet-type holder shown in Fig. 2 a) here worn by a subject in the MEG measurement position inside the MSR. The sensor positions are marked by green circles in Fig. 2 b) superimposed on the skull surface of the subject retrieved from MRI Images, which were needed for the 3D printing of the helmet. The OPM sensors are placed in such a way that all directions of space of the room are almost equally sampled and the distributions in Figs. 1 b) and c) are representative for the fluctuations in the MSR without and with active shielding.

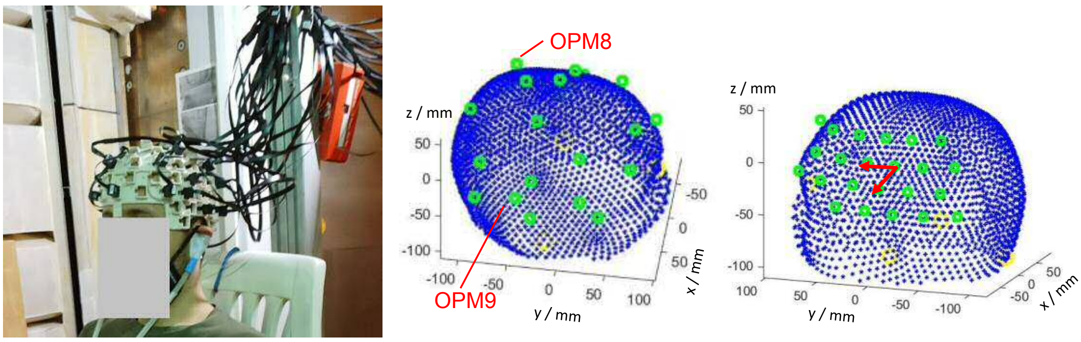

a) b) c)

Figure 2. *a) MEG setup consisting of 25 dual-axis OPM sensors (QZFM Gen 2.0) installed in the actively shielded two-layer MSR. For the MEG recording the subject listens to binaurally delivered tones and wears a 3D printed helmet designed from the individual anatomy. b) Layout of sensors evenly distributed around the head (nose is at the right side). c) Layout of sensors arranged in a grid to measure signals from the left auditory cortex with the center of the grid placed at C3 (10-20 EEG naming, nose is at the left side). The red arrows show for one sensor the sensitive directions z and y, which correspond to the quasi-radial and horizontal tangential direction of the brain field.*

Besides the sensor placement shown in Fig. 2 a) and b) a second patch like placement was used. It is shown in Fig. 2 c) and sensors were placed to measure the MEG of the left hemisphere around C3 (C3 refers to the naming convention for EEG electrodes, the 10-20 system.).

The subject was seated comfortably during the MEG measurement as can be seen in Fig. 2 a). The subject was listening passively to 1 kHz tones delivered over a tube into both ears (ER-30 etymotic.com). One tube can be seen running down from the left ear. It is attached to the blue earpiece holding the foam ear inserts.

3. Results

The recorded raw data from 50 channels (25 dual-axis sensors) were bandpass filtered between 3 and 45 Hz Hz to remove unwanted noise at lower frequencies compromising the baseline and to remove power line interference. Then the auditory evoked fields (AEF) were calculated by averaging the epochs corresponding to the 500 tone presentations. Four exemplary channels out of the 50 recorded channels are shown in Fig. 3. The selected sensors OPM8 and OPM9, one from each hemisphere, were almost symmetrically placed in the region of positions TP7 and TP8 (EEG 10-20 naming scheme) as can be seen in Fig. 2 b). Both quasi-radial (z) and tangential (y) fields show a strong peak at 100 ms, the M100 with an amplitude of 500 fT in z- and 150-400 fT in y-direction. The opposite sign between the hemispheres is a consequence of the brain current activation in both hemispheres flowing in the same direction and consequently the dipole fields change sign between hemispheres. This has been known since the first multi-channel SQUID measurements of AEF brain responses (Knuutilla et al., 1993). The weaker peak in OPM9y shows that the tangential field sees additional information beyond the quasi-radial field.

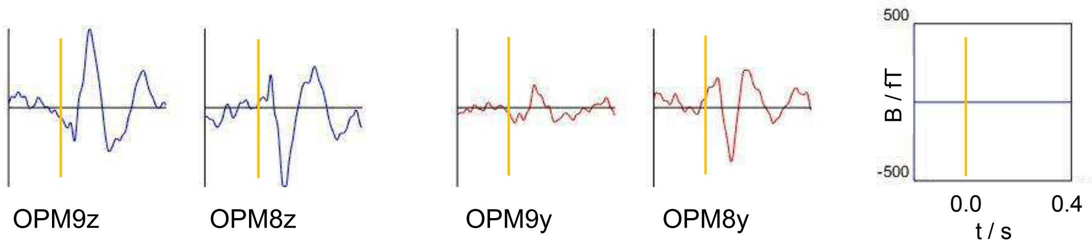

Figure 3. *AFEs for two posterior sensors one from each hemisphere as marked in Fig. 2 b). The yellow line is the time of the tone onset. Both directions z and y show a response at 100 ms known from the literature as the auditory M100. The sign of the response is opposite between the hemispheres for the quasi-radial (z-) direction as a consequence of the current running symmetrical in both auditory cortices. The tangential (y-)direction responses show an opposite sign as well, but the difference in amplitude suggest a different brain current configuration or a difference in placement of the sensors relative to the anatomy.*

The results for the patch-like sensor layout over the left hemispheric auditory cortex (Fig 2. c)) are shown as maps in Fig. 4 for three time points, at 80, 100, and 120 ms chosen to visualize the M100. A clear dipolar map can be seen at 100 ms in the z-fields consistent with the peak position at 100 ms in Fig. 3. These z-magnetometer (quasi-radial) maps are consistent with the magnetometer maps calculated in (Knuutila et al., 1993) from quasi-radial field gradients.

The z-map has a zero-line (dashed red vertical line) coinciding with the maximum of the y-map representing the tangential field in the axial plane. The relation between quasi-radial and tangential field maps was studied before using a SQUID vector magnetometer array (Haueisen et al., 2012) and particularly the tripolar map in the tangential direction is well reproduced in the OPMy map at 100 ms.

4. Discussion

Besides the active shielding by coils on the outside of the MSR demonstrated here other approaches have been explored. Using a triple axis gradient coil system enclosing thorax and head and using OPMs itself as control input for a PID controlled current source somatosensory brain responses were successfully extracted (Iivanainen et al., 2019). This method does not require any modification of the MSR and can be installed as needed. Cylindrical full body shields requiring much less μ-metal compared to an MSR need coils embedded in the cylinder to null the background fields for SERF OPM operation (Borna et al., 2020). In the cylindrical shield somatosensory and AEF responses were measured and could be localized in good agreement with SQUID-MEG results measured on the same subjects.

Here AEFs of similar quality were recorded with ease in a two-layer MSR with external active shielding. This shows the zero-field OPM-MEG readiness of our setup. Compared to the setups of (Iivanainen et al., 2019) and (Borna et al., 2020) our setup with coils on the cuboid outside is simple and can be added to existing MSRs at moderate cost. The present coils were added by the manufacturer during installation of the room but it is imaginable to upgrade an existing room even without involving a company. Nevertheless, commercial solutions have been available (Elekta AB, Sweden).

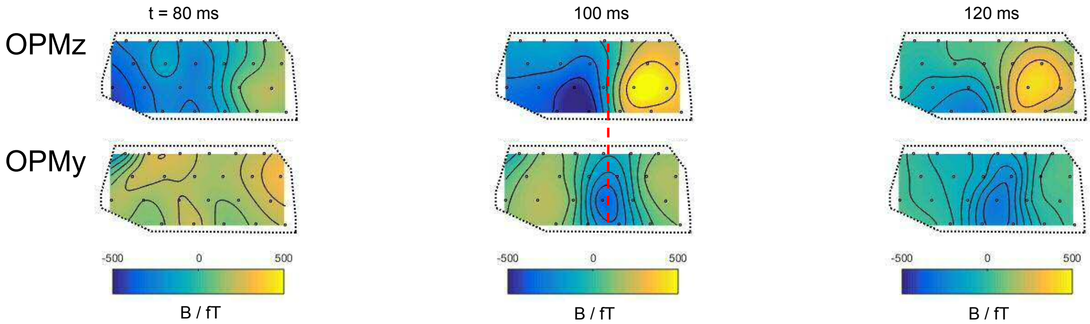

Figure 4. *Averaged field maps from 500 tone presentations showing at 100 ms the typical field map of the AEF M100 response. The array coverage is shown Fig. 2 c). It covers the left hemisphere around position C3 (EEG 10-20 naming). The orientation is identical to the layout in Fig. 2 c). Top row is the z-signal of the sensors corresponding to the quasi-radial field component, bottom row is the y-signal of the sensors showing the tangential field component. The dashed red line shows that the maximum of the tangential field is aligned with the zero line of the dipolar quasi-radial field as it is expected for a current tangential to the skull.*

5. Conclusions

The active shielding in a triple-axis configuration on the outside edges of a MSR reduces the typical urban environment field fluctuations sufficiently to operate zero-field OPM sensors in the linear regime. This was shown by the OPM signal distribution for a typical MEG recording length of 30 minutes. The OPM sensors were inserted into an individualized sensor helmet made by 3D printing to allow a very comfortable MEG recording. A drawback of our approach is the requirement to have MRI images of the subject's head. AEFs were recorded using 25 dual-axis sensors yielding 50 channels. Amplitudes and field maps are in very good agreement with literature and measuring both quasi-radial and tangential components allows to gain more information without increasing the number of sensors.

Although the active shielding coils were part of the initial design of the MSR an upgrade appears possible for other existing MSRs with such cuboid edge coils. This would preserve the considerable investment represented by an MSR and at the same time allow MEG based on zero-field OPM sensors. Future work will focus on reducing the internal static gradients to allow movements of subjects.

Acknowledgments

Support by DAAD project ID 57402032 and Slovenian Research Agency project ID P2-0348 is acknowledged. Helpful discussions with Allard Schnabel and Jens Voigt are gratefully acknowledged.

References

Borna A, Carter TR, Colombo AP, Jau YY, McKay J,Weisend M, Taulu S, Stephen JM, and Schwindt PDD (2020) Non-Invasive Functional-Brain-Imaging with an OPM-based Magnetoencephalography System. PLOS ONE 15(1), e0227684.

Boto E, Holmes N, Leggett J, Roberts G, Shah V, Meyer SS, Muñoz LD, Mullinger KJ, Tierney TM, Bestmann S, Barnes GR, Bowtell R, Brookes MJ (2018) Moving magnetoencephalography towards real-world applications with a wearable system. Nature, 555, pp. 657-661.

Haueisen J, Fleissig K, Strohmeier D, Elsarnagawy T, Huonker R, Liehr M, Witte OW (2012) Reconstruction of quasi-radial dipolar activity using three-component magnetic field measurements. Clinical Neurophysiology, 123, pp. 1581-1585.

Iivanainen J, Zetter R, Grön M, Hakkarainen K, Parkkonen L (2019) On-scalp MEG system utilizing an actively shielded array of optically pumped magnetometers. NeuroImage, 194, pp. 244-258.

Knuutila K, Ahonen A, Hamalainen M, Kajola M, Laine PP, Lounasmaa O, Parkkonen L, Simola J, Tesche C (1993) A 122-channel whole-cortex SQUID system for measuring the brain's magnetic fields. IEEE Transactions on Magnetics, 29, pp. 3315-3320.

Malmivuo J, Lekkala J, Kontro P, Suomaa L, Vihinen H (1987) Improvement of the properties of an eddy current magnetic shield with active compensation. Journal of Physics E Scientific Instruments, 20, pp. 151-164.

Marhl U, Jodko-Wladzinska A, Brühl R, Sander TH, Jazbinšek V (2021) Comparison between conventional SQUID based and novel OPM based measuring systems in MEG. *In T. Jarm et al. (Eds.): EMBEC 2020,* IFMBE Proc. 80, pp. 254–261.

Osborne J, Orton J, Alem O, Shah V (2018) Fully integrated, standalone zero field opticall pumped magnetometer for biomagnetism. *Proc. SPIE 10548, Steep Dispersion Engineering and Opto-Atomic Precision Metrology XI*, pp. 1–7.

Gross J (2019) Magnetoencephalography in Cognitive Neuroscience: A Primer. Neuron, 104, pp. 189-204.

Sander TH, Jodko-Wladzinska A, Hartwig S, Brühl R, Middelmann T (2020) Optically pumped magnetometers enable a new level of biomagnetic measurements. Adv Opt Techn, 9, pp. 247–251.